Acta Cryst. (1986). A42, 24-29

Determination of the Photoelectron Emission Probability with Inclined X-ray Laue Diffraction

BY A. M. AFANAS'EV

Kurchatov Institute of Atomic Energy, Moscow 123182, *USSR*

AND R. M. IMAMOV, E. KH. MUKHAMEDZHANOV AND A. N. CHUZO

Institute of Crystallography, USSR Academy of Sciences, 59, *Leninskii Prospekt*, 117333 *Moscow, USSR*

(*Received* 21 *January* 1985; *accepted* 18 *June* 1985)

Abstract

A simple relation has been established between the Fourier component of the probability density $P(z)$ of photoelectron emission from different depths of a crystal and the angular dependence of the emission of photoelectrons formed in inclined X-ray Laue diffraction, which for the first time permitted the use of a direct method for the reconstruction of the $P(z)$ function. Accurate measurements of the angular dependence of photoelectron emission were carried out on a silicon single crystal with diffraction of Cu K_α radiation for different energy ranges. Photoelectrons were recorded by a proportional gas counter specially designed for the energy analysis of photoelectrons under inclined Laue diffraction conditions. The laws predicted by the theory have been fully confirmed, and the corresponding $P(z)$ functions have been obtained.

1. Introduction

The knowledge of the probability of the emission of photoelectrons formed at different depths of a crystal during absorption of light, X-rays or Mössbauer γ quanta is of great importance for different fields of physics. Many authors considered this problem theoretically (Krakowskii & Miller, 1972; Liljequist, Ekdahl & Bäverstam, 1978; Liljequist & Ekdahl, 1978), and in a series of works the authors make attempts to reconstruct the $P(z)$ function experimentally (Bäverstam, Bohm, Ringström & Ekdahl, 1973; Thomas, Tricker & Winterbottom, 1975). Yet the problem is far from being solved. In principle, theoretical works permit one to calculate $P(z)$ with a very high accuracy for electrons having different energies with due account of physical processes accompanying the emission of photoelectrons from a substance. But there is no possibility to take into consideration those specific distortions that are introduced into the process of photoelectron recording. In other words, the $P(z)$ function is not only a characteristic of a substance but also that of the experimental set-up. Therefore, the problem of the experimental determination of $P(z)$ is still urgent. Lately, attempts have been made to solve the problem by the X-ray standing-wave technique (Mukhamedzhanov, Maslov, Chuzo & Imamov, 1984), yet such experiments required a large number of different specimens and, on the whole, the method proved to be very laborious.

The present work suggests for the first time a method for direct determination of $P(z)$ from the angular dependence of photoelectron emission during absorption of X-rays under the inclined Laue diffraction conditions and illustrates its experimental realization. Photoelectron emission in such diffraction geometry (Fig. 1) was studied by Afanas'ev, Imamov, Maslov & Pashaev (1983). This work showed the possible effective use of a new modification of X-ray standing waves (see Andersen, Golovchenko & Mair, 1976; Cowan, Golovchenko & Robbins, 1980, and references therein) for the analysis of structure perfection of thin crystalline films.

2. Theory

Diffraction geometry shown in Fig. 1 is not used in conventional diffraction experiments since, in fact,

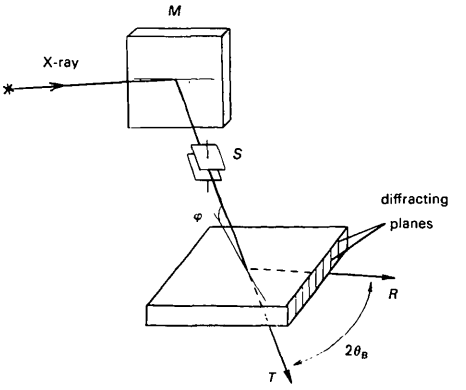

Fig. 1. Diffraction scheme: M monochromator, S slit, φ grazing incidence angle, R diffracted beam, T transmitted beam.

0108-7673/86/010024-06$01.50

© 1986 International Union of Crystallography

the tilting of a crystal leads only to an increase in its effective thickness. Yet, if photoelectron emission is measured from the entrance surface of the specimen, such a geometry turns out to be very useful. Indeed, the angular dependence of the photoelectron yield $x(\alpha)$ in such experiments is determined in the general case by two main parameters - the escape depth, L_e, and the extinction length, L_{ex}. Variation of the incidence angle φ of X-rays relative to a crystal makes it possible to change L_{ex} within a wide range. At large φ (the conventional geometry of Laue diffraction), when $L_{ex} \gg L_e$, the diffracted wave does not have enough time to form at depth L_e, the interference effects are almost absent, and $x(\alpha)$ only slightly deviates from a straight line. For smaller incidence angle φ the value of L_{ex} becomes of the order of L_e and even smaller. This fact is reflected in a sharp enhancement of interference effects leading, in turn, to an anomalous angular dependence of the photoelectron yield $x(\alpha)$ and, as was shown by Afanas'ev, Imamov, Maslov & Pashaev (1983), at $L_{ex} \leq L_e$ $x(\alpha)$ should depend on crystal perfection at depth L_e. In contrast to the conventional X-ray standing-wave technique using the Bragg diffraction geometry, the use of inclined Laue diffraction allows the possibility of measuring crystal structure parameters in crystallographic directions parallel to the surface.

In the intermediate case when $L_{ex} \sim L_e$ the shape of the $x(\alpha)$ curve already essentially depends on the particular form of the probability density $P(z)$ of photoelectron emission, which opens up a possibility of the direct determination of the $P(z)$ function.

Though the schematic diagram in Fig. 1 differs from the commonly used geometry of Laue diffraction, the diffraction process occurs as in the usual case, and we may apply the dynamical theory of X-ray diffraction to the wave fields inside the crystal (Pinsker, 1978). The electromagnetic field of an X-ray wave in a crystal has the form

$$E = E_0(\alpha, z) \exp(i\mathbf{kr}) + E_h(\alpha, z) \exp(i\mathbf{k}_h\mathbf{r}) \quad (1)$$

where

$$\begin{aligned}
E_0(\alpha, z) &= [(2\varepsilon_0^{(2)} - \chi_0)/(2\varepsilon_0^{(2)} - 2\varepsilon_0^{(1)})] \\
&\quad \times \exp(ik\varepsilon_0^{(1)} z/\gamma_0) \\
&\quad - [(2\varepsilon_0^{(1)} - \chi_0)/(2\varepsilon_0^{(2)} - 2\varepsilon_0^{(1)})] \\
&\quad \times \exp(ik\varepsilon_0^{(2)} z/\gamma_0), \\
E_h(\alpha, z) &= -[\beta\chi_h/(2\varepsilon_0^{(2)} - 2\varepsilon_0^{(1)})] \\
&\quad \times [\exp(ik\varepsilon_0^{(1)} z/\gamma_0) - \exp(ik\varepsilon_0^{(2)} z/\gamma_0)], \\
(2\varepsilon_0^{(1,2)} - \chi_0) &= \tfrac{1}{2}(-\beta\alpha - \chi_0(1-\beta) \\
&\quad \pm \{[\chi_0(1-\beta) + \beta\alpha]^2 + 4\beta\chi_h\chi_{\bar{h}}\}^{1/2}), \\
\alpha &= (k_h^2 - k^2)/k^2 = -2 \sin 2\theta_B \times \Delta\theta,
\end{aligned}$$

$\Delta\theta$ being the deviation from the exact Bragg angle, θ_B. $\beta = \gamma_0/\gamma_h$, γ_0 and γ_h are the cosines between the wave vectors $\mathbf{k}$ and $\mathbf{k}_h$ and the inner normal to the crystal entrance surface. $\chi_{0,h} = \chi_{r0,h} + i\chi_{i0,h}$; $\chi_{r0,h}$ and $\chi_{i0,h}$ are the real and imaginary parts of the Fourier component of polarizability. All the other symbols correspond to those of Afanas'ev & Kohn (1978).

According to the results obtained by Afanas'ev & Kohn (1978), we have for photoelectron yield:

$$x(\alpha) = \int_0^\infty P(z) x(\alpha, z)\, dz, \quad (2)$$

$$\begin{aligned}
x(\alpha, z) &= (1/\gamma_0)\{|E_0(\alpha, z)|^2 + |E_h(\alpha, z)|^2 \\
&\quad + 2 \operatorname{Re} \epsilon_h E_0^*(\alpha, z) E_{\bar{h}}(\alpha, z)\};
\end{aligned}$$

where

$$\epsilon_h = \chi_{ih} C_{\sigma,\pi}/\chi_{i0},$$

$$C_{\sigma,\pi} = \begin{cases} 1 & \text{for } \sigma \text{ polarization} \\ \cos 2\theta_B & \text{for } \pi \text{ polarization.} \end{cases}$$

Unlike diffraction in Bragg geometry, in this case we deal with two, and not one, standing waves, which are coherent. This makes it necessary to take into account phase relationships between these waves.

Near the surface, where X-ray absorption may be neglected, we arrive at the following simple expressions for the fields $E_{0,h}(\alpha, z)$:

$$\begin{aligned}
E_0(\alpha, z) &= \exp\{(ikz/\gamma_0)(\chi_0 - \tfrac{1}{2}\tilde{\alpha}_r)\} \\
&\quad \times [\cos(\Lambda_r kz/4\gamma_0) \\
&\quad + i(\tilde{\alpha}_r/\Lambda_r) \sin(\Lambda_r kz/4\gamma_0)], \\
E_h(\alpha, z) &= \exp\{(ikz/\gamma_0)(\chi_0 - \tfrac{1}{2}\tilde{\alpha}_r)\} \\
&\quad \times (2i\beta\chi_h/\Lambda_r) \sin(\Lambda_r kz/4\gamma_0),
\end{aligned} \quad (3)$$

where

$$\begin{aligned}
\Lambda_r &= \operatorname{Re}(\tilde{\alpha}_r^2 + 4\beta\chi_h\chi_{\bar{h}})^{1/2}, \\
\tilde{\alpha}_r &= \beta\alpha + \chi_{r0}(1-\beta).
\end{aligned}$$

Formulae (3) describe *Pendellösung*, an effect known from the theory of X-ray diffraction.

In accordance with (3), the angular dependence of photoelectron yield from the entrance surface of the crystal is determined by the expression

$$\begin{aligned}
x(\alpha) &= 1 + 2\beta[\operatorname{Re}(\epsilon_h\chi_{r\bar{h}})\tilde{\alpha}_r + (\beta-1)\chi_{rh}\chi_{r\bar{h}}]/\Lambda_r^2 \\
&\quad \times [1 - \langle\cos(\Lambda_r kz/2\gamma_0)\rangle] \\
&\quad + 2\beta[\operatorname{Im}(\epsilon_h\chi_{r\bar{h}})/\Lambda_r]\langle\sin(\Lambda_r kz/2\gamma_0)\rangle,
\end{aligned} \quad (4)$$

where

$$\langle \ldots \rangle = \int_0^\infty \ldots P(z)\, dz.$$

In crystals built by atoms of one kind and possessing a center of inversion (*i.e.* in Si- and Ge-type crystals)

the quantity $\epsilon_h\chi_{r\bar{h}}$ is real. Then (4) is simplified to

$$x(\alpha)=1+2\beta[(\epsilon_h\chi_{r\bar{h}})\tilde{\alpha}_r+(\beta-1)\chi_{rh}^2]/(\tilde{\alpha}_r^2+4\beta\chi_{rh}^2)\times\{1-\langle\cos[(\tilde{\alpha}_r^2+4\beta\chi_{rh}^2)^{1/2}kz/2\gamma_0]\rangle\}. \quad (5)$$

The latter expression may be rewritten as

$$x(y)=1+\{[-2\epsilon_h y\beta^{1/2}+(\beta-1)]/2(y^2+1)\}\times[1-\langle\cos[(y^2+1)^{1/2}2z/L_{ex}]\rangle], \quad (6)$$

where $L_{ex}=2(\gamma_0\gamma_h)^{1/2}/k|\chi_{rh}|C_{\sigma,\pi}$ is the so-called extinction length and $y=\tilde{\alpha}_r/2\beta^{1/2}|\chi_{rh}|C_{\sigma,\pi}$. The diffraction geometry under consideration permits one to vary angle φ, and hence parameter γ_0 and, consequently, the extinction length L_{ex}.

At large incidence angles φ the extinction length L_{ex} is usually much larger than the escape depth L_e and hence $\cos[(y^2+1)^{1/2}2z/L_{ex}]$ can be expanded into a series in the region $|y|\leq 1$:

$$x(y)=1-\epsilon_h y\sum_n(-1)^{n/2-1}\times[2^n(y^2+1)^{n/2-1}/n!L_{ex}^n]\langle z^n\rangle, \quad (n=2,4,6,\ldots). \quad (7)$$

(For simplicity, here and below it is assumed that $\beta=1$.) Here $\langle z^n\rangle$ are the corresponding moments of the function $P(z)$, which means that the slope of the $x(y)$ curve at point $y=0$, and its derivatives provide the direct determination of the most important characteristics of $P(z)$. Indeed, taking into account that $L_e/L_{ex}\ll 1$, we have

$$\left.\begin{aligned}dx/dy_\sigma&=-[(1+C_\pi^3)/(1+C_\pi)](2\epsilon_{h,\sigma}/L_{ex,\sigma}^2)\langle z^2\rangle\\ d^3x/dy_\sigma^3&=[(1+C_\pi^5)/(1+C_\pi)](4\epsilon_{h,\sigma}/L_{ex,\sigma}^4)\langle z^4\rangle\end{aligned}\right\} \quad (8)$$

etc.

The derived expressions take account of the fact that a nonpolarized X-ray wave falls onto a monochromator. If one of the polarizations is excluded (by the appropriate choice of such an order of reflection that $C_\pi=\cos 2\theta_B=0$), then it may readily be seen that (6) directly determines the Fourier component of the $P(z)$ function:

$$F(\omega)=\int_0^\infty P(z)\cos(\omega z)\,dz=[(x-1)(y^2+1)/\epsilon_h y]+1, \quad (9)$$

where $\omega=2(y^2+1)^{1/2}/L_{ex}$.

It is worth noting that moments $\langle z^n\rangle$ and $F(\omega)$ can be determined from different $x(y)$ curves corresponding to different incidence angles φ. If we change the scale, *i.e.* pass from y to ω, then in all the cases we should obtain the same values of $\langle z^n\rangle$ and the same function $F(\omega)$ for electrons from a certain energy range. This is the most important feature of the phenomenon in perfect crystals and its confirmation seems to be the main aim of the experiment. In the limiting case, $L_e\gg L_{ex}$, *i.e.* at small φ, the term with $\langle\cos[(y^2+1)^{1/2}2z/L_{ex}]\rangle$ is eliminated and we arrive at the simple expression for $x(y)$:

$$x(y)=1+[-2\epsilon_h y\beta^{1/2}+(\beta-1)]/2(y^2+1). \quad (10)$$

This expression is independent of the details of the electron escape from a crystal. Yet the experimental verification of the formula may be used as a preliminary estimate of crystal perfection. [Note here that at very small φ angles, when absorption of X-rays is already an essential process, (10) is not valid any more. In this limit $x(y)$ degenerates into a straight line.] But we made measurements at such φ angles that absorption at depth L_e could *a priori* be neglected.

As follows from (10), $x(y)=1$ at

$$y_0=(1-\beta)/2\epsilon_h\beta^{1/2}, \quad (11)$$

i.e. the photoelectron yield becomes comparable with the background level. It should be noted that it is at this value of y_0 that anomalous absorption of X-rays (the Borrmann effect) is realized. This fact may be used for precise measurements of spacings in a thin subsurface layer with a thickness of the order of L_e. Indeed, if spacings in this layer and in the matrix are different, the values of y_0 determined from the photoemission curve and from the position of the diffracted-wave peak should also be different. The difference in the y_0 values would determine a relative change of spacings in the subsurface layer.

3. Experimental

The problem of direct $P(z)$ reconstruction from an angular dependence of the photoelectron yield requires an elimination of one polarization and a precise collimation of an X-ray beam to avoid the 'convolution-type' distortions. To meet these requirements we used (Fig. 1) a strongly asymmetric Si(422) monochromator ($\theta_B=44°$ for Cu $K\alpha$ radiation, $C_\pi\simeq 0$). This resulted in the collimation of an incident beam of $\sim 1/6$ of the 422 natural reflection width. The vertical divergence of the incident beam was 5′. The specimen was a silicon wafer 4×4 cm, 300 μm thick, with the (111) planes parallel to the surface. The surface was first polished chemically and mechanically and etched to remove a possibly disturbed layer. The thickness of the residual oxide layer on the surface, not exceeding 30 Å, was measured by the method of X-ray diffraction in the grazing geometry (Aleksandrov, Afanas'ev, Melkonyan & Stepanov, 1984; Golovin & Imamov, 1983; Golovin, Imamov & Stepanov, 1984). The specimen was placed in a specially designed gas-flow proportional detector described elsewhere (Mukhamedzhanov & Le cong Qui, 1985), which recorded the photoelectron emission from the entrance surface under the Laue-

diffraction conditions at different (including grazing) incidence angles of X-rays.

The studied crystal was scanned for an hour in the Laue geometry near the exact value of the Bragg angle. During scanning, the angular dependence of the photoeffect and the 422 reflection of Cu $K\alpha$ radiation were simultaneously registered at an angular resolution of 0·07″. The number of scans varied, depending on the energy range, from two to ten to provide the necessary statistics. In addition, in each cycle we also measured the photoelectron yield far from the exact Bragg angle. Then, for corresponding energy ranges, the results of scanning were summed up, the center of the diffraction reflection curve being used as a reference point. The statistical error of the experimental data did not exceed 0·4%.

Fig. 2 shows the experimental angular curves of photoelectron emission for electrons with a given energy for two different incidence angles (a) and for electrons from two different energy ranges at a given incidence angle (b). The shape of the curves is determined by the relation between the extinction length L_{ex} and the depth L_e from which the photoelectrons escaped. In our experiment L_{ex} could be varied within a wide interval by changing the incidence angle φ, while L_e was altered by choosing the electron energy.

Fig. 3 presents the angular dependence of the emission of photoelectrons with energies $E \geq 2{\cdot}3$ keV recorded at the incidence angle $\varphi = 1{\cdot}5°$, when the dependence $x(y)$ reaches the asymptotic limit described by (10). The experimental results agree quite well with the theory, which shows the high perfection of the crystal.

4. Reconstruction of $P(z)$

According to the above theoretical analysis, the moments $\langle z^n \rangle$ of the function $P(z)$ can be readily obtained from experimental data. To determine the moments we should not necessarily have only one polarization and a very strictly collimated beam. This makes complicated schemes with the use of asymmetric monochromators unnecessary. The corresponding procedure was realized by Afanas'ev, Imamov & Mukhamedzhanov (1984*a*, *b*) for the 220 reflection and an incident with low beam collimation. In the present work, we repeated similar measurements for the 422 reflection using better collimation and obtained $\langle z^2 \rangle$ and $\langle z^4 \rangle$ for electrons from different energy ranges. To do this it was sufficient to measure only the central portions of the $x(y)$ curves at different incidence angles φ to find $x^1\varphi^2$ and $(\langle z^2 \rangle - x^1\varphi^2)\varphi^2$.

Fig. 4 depicts the corresponding curves for electrons from one energy range. (For convenience, differentiation was carried out over $\Delta\theta$.) The asymptotic value of $x^1\varphi^2$ at large φ, according to (8), gives directly $\langle z^2 \rangle$, whereas $(\langle z^2 \rangle - x^1\varphi^2)\varphi^2$ gives the value of $\langle z^4 \rangle$. Such a procedure was used for electrons from different energy ranges, and the obtained results coincided within 10% with the data previously

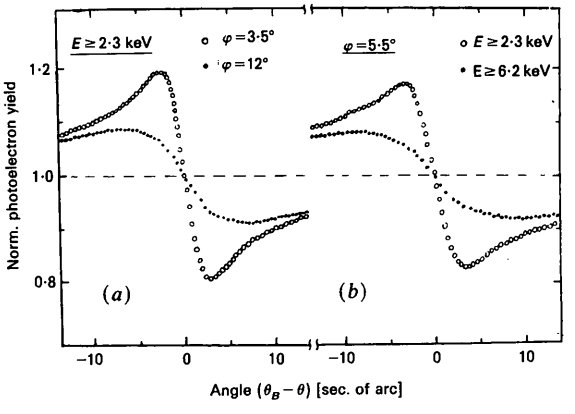

Fig. 2. Experimental angular dependence of photoelectron yield in the inclined Laue diffraction condition. Si(422) reflection, Cu $K\alpha$ radiation. (a) At a fixed electron energy; (b) at a fixed incidence angle of X-ray radiation.

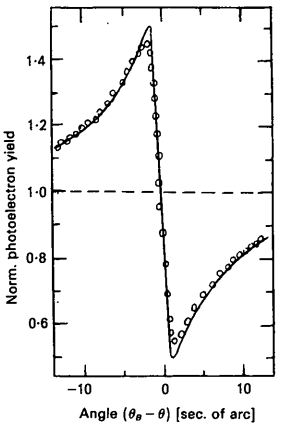

Fig. 3. Experimental (circles) angular dependence of the yield of photoelectrons with $E \geq 2{\cdot}3$ keV at the X-ray incidence angle $\varphi = 1{\cdot}5°$. The solid curve is calculated with (10) (see text); Si(422) reflection, Cu $K\alpha$ radiation.

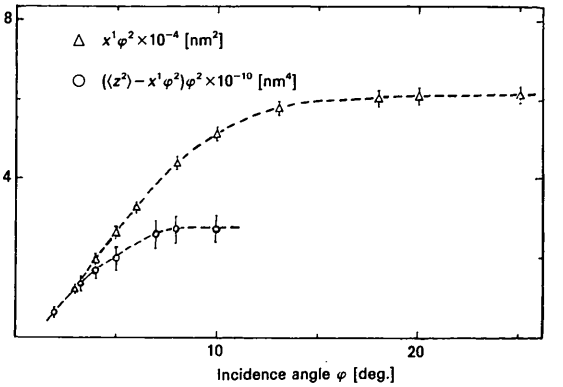

Fig. 4. Dependence of $x^1\varphi^2$ (triangles) and $(\langle z^2 \rangle - x^1\varphi^2) \cdot \varphi^2$ (circles) on the incidence angle φ of X-rays for photoelectrons with energies $E \geq 2{\cdot}3$ keV.

obtained by Afanas'ev, Imamov & Mukhamedzhanov (1984*a*, *b*). Yet the determination of the first moments of $P(z)$ still cannot be regarded as a solution of the problem, and to reconstruct $P(z)$ it is necessary, according to the above analysis, to measure experimental $x(y)$ curves without π polarization at a sufficiently high collimation of the incident beam. Such measurements were performed, and Fig. 5 shows the $F(\omega)$ function calculated from experimental $x(y)$ curves by (9). For electrons within the given energy range, the photoelectron yield for different incidence angles will give different values (see, for example, Fig. 2), but the functions $F(\omega)$ calculated from different $x(y)$ curves should coincide since they are the Fourier components of one function, $P(z, E)$. This is illustrated by Fig. 5(*a*), which depicts experimental $F(\omega)$ functions for electrons with $E \geq 2{\cdot}3$ keV and for three different incidence angles (for clarity, only some experimental points are shown). Different portions of $F(\omega)$ are described best at different values of φ, which is due to two facts. As is seen from (9), $\omega > 0$ and $\omega_{\min} = 2/L_{ex} \simeq 2/\varphi$ at any values of y. Therefore, the angular dependence obtained at a large value of φ would describe better the initial portions of $F(\omega)$ (at small ω). The second fact is that at large ω the error $\Delta F(\omega) \simeq \omega L_{ex} \simeq \omega\varphi$ increases with φ. Therefore to find $F(\omega)$ at large ω it is desirable to measure $x(y)$ curves at incidence angles as small as possible. It is seen from Fig. 5(*a*) that the data obtained at $\varphi = 16°$ describe best the initial portions of $F(\omega)$. The results corresponding to the incidence angle $\varphi = 5°$ permit one to follow the run of $F(\omega)$ up to much larger values of ω. For the portions where the data overlap one should naturally use the information from several curves, which provides the lowest possible error.

The behavior of $F(\omega)$ at small ω can be obtained from the experiment by measuring the angular dependence of the photoeffect at large φ. But, in fact, there is no necessity to do so. The function $F(\omega)$ at $\omega z \ll 1$ can be represented in the form

$$F(\omega) = \int_0^\infty P(z)(1 - \tfrac{1}{2}\omega^2 z^2)\,dz = 1 - \tfrac{1}{2}\omega^2\langle z^2\rangle, \qquad (12)$$

i.e. at small values of ω, $F(\omega)$ is described by a parabola; the parameter $\langle z^2\rangle$ can readily be determined directly from the experiment by the above procedure. The dependence (12) is depicted by a dashed line in Fig. 5. From Fig. 5(*b*), where the initial portion of the $F(\omega)$ curve is shown on a larger scale, it is seen that points obtained at $\varphi = 16°$ lie on the portion described by (12). Obviously, there is no need to measure photoemission curves at large φ since such data would not contain any new information.

Fig. 6(*a*) shows similar curves for electrons with energies $E \geq 5{\cdot}5$ keV obtained for two incidence angles φ. As should be expected, the initial portion of $F(\omega)$ for electrons having a higher energy and a smaller escape depth is described by (12) at essentially smaller values of φ.

The behaviour of $F(\omega)$ at large ω is also approximated by a rather simple expression. Integrating by parts the integral in (9), taking into account that $P(\infty) = 0$, we obtain

$$F(\omega) \underset{\omega\to\infty}{=} -P'(0)/\omega^2, \qquad (13)$$

where

$$P'(0) = dP(z)/dz|_{z=0}.$$

Fig. 6(*b*) shows the run of $F(\omega)$ at large ω (the inset shows all the experimental points) and the least-squares approximation of $F(\omega)$ by expression (13). As a result of the above simple procedure, we can determine the first derivative $P'(0)$ of the function $P(z)$.

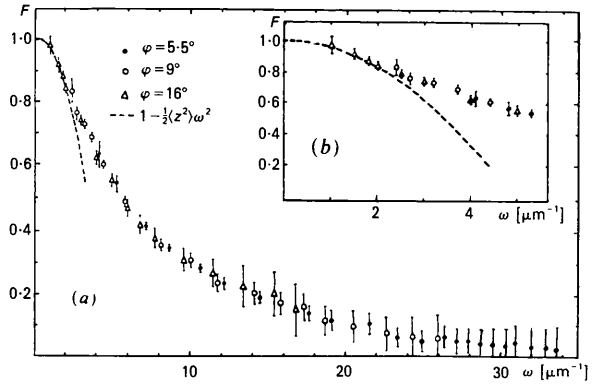

Fig. 5. (*a*) Fourier component $F(\omega)$ of the function of the emission probability for photoelectrons with energy $E \geq 2{\cdot}3$ keV obtained for incidence angles $\varphi = 5{\cdot}5°$ (points), $\varphi = 9°$ (circles), $\varphi = 16°$ (triangles) (silicon, Cu $K\alpha$ radiation). The dashed line shows the dependence $1 - \frac{1}{2}\omega^2\langle z^2\rangle$. (*b*) Behavior of $F(\omega)$ at small ω.

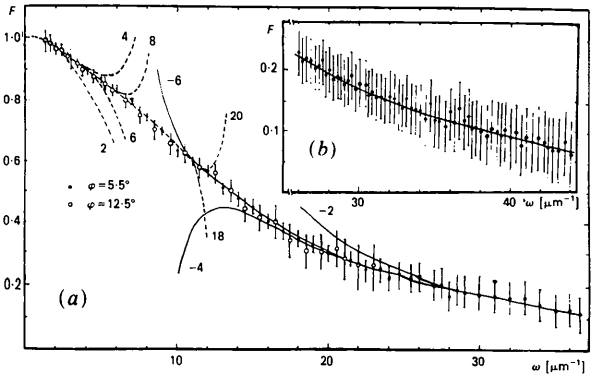

Fig. 6. (*a*) Fourier component $F(\omega)$ of the function of emission probability for photoelectrons with energies $E \geq 5{\cdot}5$ keV obtained at the incidence angles of X-rays $\varphi = 5{\cdot}5°$ (points) and $\varphi = 12{\cdot}5°$ (circles) (silicon, Cu $K\alpha$ radiation). The dashed line is the approximation of $F(\omega)$ by the expression $1 - \sum_{k=1}^{n} b_k\omega^{2k}$ at $n = 1, 2, 3, 4, 10$. The solid line is the approximation of $F(\omega)$ by the expression $\sum_{k=1}^{m} a_k\omega^{-2k}$ at $m = 1, 2, 3$. (The figures on the approximation curves are the powers of ω.) (*b*) Behavior of $F(\omega)$ at large values of ω.

In the general form (13) can be written as

$$F(\omega) \underset{\omega\to\infty}{=} \sum_k a_k \omega^{-2k}, \quad (k=1,2,3,\ldots), \qquad (14)$$

where

$$a_k = (-1)^k \cdot P^{(2k-1)}(0).$$

Fig. 6(a) represents the results of the $F(\omega)$ approximation at large ω taking into account one, two and three terms of the sum in (14). We have thus found the function $F(\omega)$ within the whole range of the argument variation. The middle part ($\omega_{\min} < \omega < \omega_{\max}$) comes from experimental points obtained for two-three different incidence angles φ, the side portions of the curve were constructed with the approximations (12) and (13).

Approximation of $F(\omega)$ at small ω was carried out taking into account terms containing ω^{2k} up to $k=10$ (Fig. (6a)). In a similar way, we determined the functions $F(\omega)$ for electrons from other energy ranges.

As has already been noted, $F(\omega)$ is a Fourier component of the function $P(z)$. Thus, $P(z)$ can be found by an inverse cosine Fourier transformation:

$$P(z) = 2/\pi \int_0^\infty F(\omega) \cos(\omega z)\, d\omega. \qquad (15)$$

Thus, reconstructed $P(z)$ functions for electrons from different energy ranges are depicted in Fig. 7.

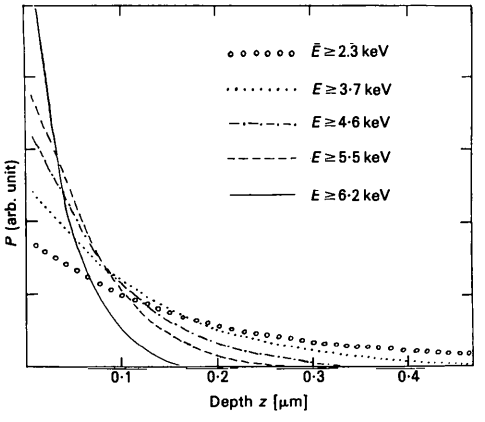

Fig. 7. The functions of the photoelectron emission probability $P(z)$ for electrons with different energies (silicon, Cu $K\alpha$ radiation).

With the variation in the energy of electrons, E, $P(z, E)$ curves change in accordance with the physical concepts on the mechanisms of photoelectron emission from a crystal. Electrons with higher energies escape from smaller depths. The typical escape depths agree with existing theoretical concepts (see, for example, Liljequist, Ekdahl & Bäverstam, 1978). We are not going to invoke here theoretical models and make detailed comparison between the theory and experiment. As has already been indicated, the functions $P(z, E)$ are determined not only by the properties of a crystal but also by the characteristics of the spectrometers used. Our aim was, in fact, to prove the possibility of the direct $P(z, E)$ determination on the basis of the analysis of specific features of the experiment without invoking any theoretical models.

References

AFANAS'EV, A. M., IMAMOV, R. M., MASLOV, A. V. & PASHAEV, E. M. (1983). *Dokl. Akad. Nauk SSSR* **273**, 609-612.

AFANAS'EV, A. M., IMAMOV, R. M. & MUKHAMEDZHANOV, E. KH. (1984*a*). *Phys. Status Solidi A*, **83**, K5-K9.

AFANAS'EV, A. M., IMAMOV, R. M. & MUKHAMEDZHANOV, E. KH. (1984*b*). *Fiz. Tverd. Tela*, **26**, 1976-1980.

AFANAS'EV, A. M. & KOHN, V. G. (1978). *Zh. Eksp. Teor. Fiz.* **74**, 300-313.

ALEKSANDROV, P. A., AFANAS'EV, A. M., MELKONYAN, M. K. & STEPANOV, S. A. (1984). *Phys. Status Solidi A*, **81**, 47-53.

ANDERSEN, S. K., GOLOVCHENKO, J. A. & MAIR, G. (1976). *Phys. Rev. Lett.* **37**, 1141-1146.

BÄVERSTAM, U., BOHM, C., RINGSTRÖM, B. & EKDAHL, T. (1973). *Nucl. Instrum. Methods*, **108**, 439-443.

COWAN, P. L., GOLOVCHENKO, J. A. & ROBBINS, M. F. (1980). *Phys. Rev. Lett.* **44**, 1680-1683.

GOLOVIN, A. L. & IMAMOV, R. M. (1983). *Phys. Status Solidi A*, **80**, K63-K65.

GOLOVIN, A. L., IMAMOV, R. M. & STEPANOV, S. A. (1984). *Acta Cryst.* A**40**, 225-227.

KRAKOWSKII, R. A. & MILLER, R. B. (1972). *Nucl. Instrum. Methods*, **100**, 93-105.

LILJEQUIST, D. & EKDAHL, T. (1978). USIP-Report No. 17.

LILJEQUIST, D. EKDAHL, T. & BÄVERSTAM, U. (1978). *Nucl. Instrum. Methods*, **155**, 529-537.

MUKHAMEDZHANOV, E. KH. & LE CONG QUI (1985). *Prib. i Tekh. Eksp.* In the press.

MUKHAMEDZHANOV, E. KH., MASLOV, A. V., CHUZO, A. N. & IMAMOV, R. M. (1984). *Poverkhnost'*, **3**, 54-59.

PINSKER, Z. G. (1978). *Dynamical Scattering of X-rays in Crystals*, pp. 32-60. Berlin: Springer-Verlag.

THOMAS, J. M., TRICKER, M. J. & WINTERBOTTOM, A. P. (1975). *J. Chem. Soc. Faraday Trans.* 2, **71**, 1708-1719.